doi.org/10.36721/PJPS.2026.39.7.187.1

Integrated analysis of single-cell and bulk-RNA sequencing data reveals drug therapeutic targets and prognostic biomarkers related to ribosome biogenesis in hepatocellular carcinoma

Anjing Zhao, Jinglian Zheng, Jingjing Feng, Xiaoqu Zhu, Linrong Zhu, Qianqian Hu and Chunming Wu*

Hepatic Department, Wenzhou TCM Hospital of Zhejiang Chinese Medical University, Wenzhou, Zhejiang, China

Abstract: **Background**: Ribosome biogenesis is involved in the progression of hepatocellular carcinoma (HCC), but the specific mechanisms and diagnostic values of ribosome biogenesis-related genes (RBRGs) in HCC remain unclear. **Objectives**: We aimed to explore potential therapeutic targets in HCC from RBRGs. **Methods**: The differentially expressed RBRGs (DE-RBRGs) were explored using publicly available bulk RNA-sequencing data. Cox regression analysis was employed to evaluate the prognostic significance of the DE-RBRGs. The optimal machine learning algorithm was selected to construct a prognostic model. The predictive performance of the model was assessed using Kaplan-Meier analysis and receiver operating characteristic (ROC) curves. Single-cell RNA-sequencing data were subsequently utilized to identify key cell populations and the corresponding DE-RBRGs. **Results**: Bioinformatics analyses revealed 88 DE-RBRGs, predominantly enriched in ribosome biogenesis-related functions and pathways. The univariate Cox regression identified 12 DE-RBRGs with prognostic values. Following, the optimal machine learning algorithm (StepCox [forward] + SuperPC) was selected to construct a prognostic model. Survival analysis demonstrated that patients in the low-risk group exhibited markedly prolonged lifespan relative to their high-risk counterparts. ROC curves confirmed the predictive accuracy of this prognostic model in both training and validation cohorts. These 12 DE-RBRGs were significantly associated with immune cell infiltration, tumor immune evasion and drug sensitivity. Analysis of single-cell sequencing data identified hepatocytes as central mediators of HCC pathogenesis, which was associated with high expression of two DE-RBRGs: Nucleophosmin 1 (*NPM1*) and Ras-Related Nuclear Protein (*RAN*). **Conclusion**: *NPM1* and *RAN*, which are highly expressed in hepatocytes, may serve as potential therapeutic targets in HCC. Their established roles in ribosome biogenesis could drive the development of novel therapies targeting this pathway.

Keywords: Hepatocellular carcinoma; Machine learning; Ribosome biogenesis-related genes; Single-cell analysis; Therapeutic targets; Validation analysis

Submitted on 23-06-2025 – Revised on 05-09-2025 – Accepted on 08-09-2025

INTRODUCTION

Hepatocellular carcinoma (HCC) is one of the most prevalent primary hepatic malignancies worldwide (Dopazo *et al*., 2024). Despite substantial advancements in clinical diagnostic and therapeutic technologies in recent years (including targeted therapies, immunotherapy and precision medicine) the overall five-year survival rate of patients with HCC remains below 30% (Brown *et al*., 2023, Wang and Deng, 2023). This poor prognosis severely affects the quality of life and survival prospects of patients. Therefore, elucidating the underlying cellular mechanisms driving HCC progression and identifying predictive biomarkers are essential to improve therapeutic efficacy (Chan *et al*., 2024).

Ribosome biogenesis, a highly complex cellular process, serves not only as the cornerstone of protein synthesis but also as a critical regulator of cell proliferation, differentiation and stress responses (Ni and Buszczak, 2023). Recent studies have revealed the essential role of ribosome biogenesis-related genes (RBRGs) in the pathogenesis of human diseases (Wang *et al*., 2024b). Among various modulators involved in ribosomal synthesis, HEAT Repeat-Containing 1 (*HEATR1*) exhibited the most pronounced upregulation in hepatic tumor specimens (Yang *et al*., 2023), functioning as a pivotal regulator of ribosome assembly and proteostasis to promote hepatic oncogenesis. Similarly, Mitochondrial Ribosomal Protein L12 (*MRPL12*) potentiates HCC by regulating mitochondrial biogenesis and metabolic reprogramming (Ji *et al*., 2024). As a nuclear component involved in ribosomal DNA regulation, Treacle Ribosome Biogenesis Factor 1 (*TCOF1*) facilitates malignant signaling and ribosomal RNA synthesis to accelerate HCC progression (Wu *et al*., 2022). These studies indicate close relationships between RBRGs and the development of HCC, highlighting the importance of further mechanistic exploration.

Advances in single-cell sequencing technologies have enabled us to explore the regulatory roles of ribosome biogenesis in HCC progression from a novel perspective (Zhang *et al*., 2023b). Notably, RBRGs have emerged as valuable biomarkers for the diagnosis and prognosis of human cancers. For instance, Roy *et al*. indicated that *PNO1* could be used as a diagnostic and prognostic biomarker for HCC, with its knockout offering therapeutic benefits (Roy *et al*., 2024). Liu *et al*. showed that

**Corresponding author:* e-mail: wuchunming9999@163.com

SNORA23 exhibited antitumor effects in HCC and could be used as a diagnostic marker for HCC (Liu *et al*., 2021b). However, the specific mechanisms and diagnostic values of RBRGs in HCC remain unclear.

In this study, the complex regulatory mechanisms and heterogeneous expression patterns of ribosome biogenesis in HCC were comprehensively elucidated by integrating bulk and single-cell transcriptomic datasets. We also validated this RBRG-based prognostic model using independent cohorts. Our findings provide new theoretical foundations and potential therapeutic targets for the precise treatment of HCC, with significant clinical implications for advancing personalized HCC therapy.

MATERIALS AND METHODS

Microarray data and data preprocessing

Bulk RNA-seq data of The Cancer Genome Atlas (TCGA)-LIHC and associated clinical information from 375 HCC samples and 50 normal samples were obtained from TCGA database and used as the training dataset in the current study. In addition, three bulk RNA datasets, the International Cancer Genome Consortium (ICGC, 243 HCC samples), GSE14520 (Wu *et al*., 2023) (225 HCC and 220 normal samples) and GSE76427 (Grinchuk *et al*., 2018) (115 HCC and 52 normal samples), were used for the external validation analysis. The scRNA dataset GSE149614 (Li *et al*., 2024), including 10 HCC and 9 normal samples, was used for single-cell analysis.

For the transcriptomic data derived from TCGA, we applied the variance stabilizing transformation method using DESeq2::vst, followed by data normalization to reduce heterogeneity. For the Gene Expression Omnibus (GEO) database, the raw data were downloaded using the GEOquery package, and the sample information was obtained via the pData function. Data correction was implemented using the normalize Between Arrays function from the limma package. If the maximum value of the data exceeded 100, log2 transformation (log2[exp + 1]) was applied.

Differential expression analysis

Based on the article published by Zang *et al*., 331 genes involved in the regulation of ribosome biogenesis were identified as RBRGs (Zang *et al*., 2024). The expression levels of these RBRGs were quantified into a gene set variation analysis (GSVA) score for each sample using ssGSEA methodology to assess the involvement of ribosome biogenesis. The differentially expressed genes (DEGs) between HCC and normal samples were explored using the DESeq2 package in R (Love *et al*., 2014) with the default dispersion estimation approach (blind method) to ensure robustness of the analysis. Genes exhibiting a Benjamini-Hochberg-corrected P value below 0.05 coupled with an absolute $\log_2$fold change (FC) exceeding 1 were identified as DEGs. The intersection between the DEGs and RBRGs was defined as differentially expressed RBRGs (DE-RBRGs).

Enrichment and protein-protein interaction (PPI) analyses

Gene Ontology (GO) function and Kyoto Encyclopedia of Genes and Genomes (KEGG) pathway enrichment analyses were performed on DE-RBRGs using the clusterProfiler package in R (Rosell-Díaz *et al*., 2024). The GO functions included biological processes (BPs), cellular components (CCs) and molecular functions (MFs). Results with $P < 0.05$ were considered statistically significant.

According to the STRING database (version: 11.0) (Szklarczyk *et al*., 2016), the PPI pairs among DE-RBRGs were predicted with a score > 0.9. The molecular interaction network was then visualized using Cytoscape platform (version: 3.7.1) (Wu *et al*., 2021).

Prognostic genes analysis

Univariate Cox regression was applied to DE-RBRGs to identify prognostic genes using the survival package in the R software (Liu *et al*., 2021a). In addition, a PPI network was constructed based on these prognostic genes using Gene MANIA (Warde-Farley *et al*., 2010), followed by functional prediction of core genes within the PPI network.

Prognostic model construction and validation

Based on the prognostic DE-RBRGs, we employed the ML.Dev.Prog.Sig function from the Mime1 package to train and validate the prognostic model in TCGA, ICGC and GSE14520 datasets. This methodology, originally developed by Liu *et al*. (Liu *et al*., 2024), integrates 101 machine learning algorithms, including both individual and ensemble models. It employs ten-fold cross-validation to fit these 101 predictive models and calculates the concordance index (C-index) for both training and validation sets, thereby identifying the optimal strategy for constructing a prognostic model. Subsequently, a DE-RBRG-based prognostic model was developed by assigning risk scores to each sample. The study population was then stratified into two subgroups according to their risk scores, using the median value as the cutoff point for each dataset. Kaplan-Meier (KM) curves were generated using the R survminer toolkit package to assess survival differences between these subgroups. Receiver operating characteristic (ROC) curves were constructed using the timeROC v0.4 package (Yu *et al*., 2023a) to evaluate the model's predictive specificity and sensitivity. Furthermore, a univariate meta-analysis was performed using the meta_unicox_vis function in the Mime1 package to test the effect of the prognostic model on HCC prognosis. Finally, the expression patterns and survival relevance of all the prognostic genes were validated in two independent external cohorts: GSE14520 and GSE76427.

Immune landscape and drug sensitivity analyses

To characterize the tumor immune microenvironment, we employed the single-sample gene set enrichment analysis

(ssGSEA) methodology (Xiao *et al*., 2020) to quantify infiltration levels of 28 immune cell subsets across different risk groups. Relationships between the prognostic genes and immune cell infiltration were determined using Spearman's correlation analysis. Additionally, we evaluated potential differences in immune evasion capacity between the risk groups by calculating tumor immune dysfunction and exclusion (TIDE) scores for individual cases. The expression variations of multiple immune checkpoint molecules, including CD274, PDCD1 and CTLA4, across the risk groups were also examined. Genomic instability was quantified by calculating tumor mutation burden values from TCGA mutation profiles using Maftools software (version: 2.18.0) and visualized using a waterfall plot. Correlations between the prognostic genes and drug sensitivity were predicted using the GSCALite database.

Single-cell data preprocessing

Data pre-processing was performed based on the GSE149614 dataset. Briefly, quality control (QC) was performed using the PercentageFeatureSet, VlnPlot and FeatureScatter functions in the R. Seurat package to filter high-quality cells. The QC criteria were as follows: nFeature_RNA between 200 and 8,000, nCount_RNA between 200 and 50,000 and percent.mt (mitochondrial gene percentage) < 15%. Subsequently, the data were log-normalized using the NormalizeData function and scaled to 10,000 UMIs per cell. Batch effect correction was performed using the RunHarmony function in the R. harmony package. Next, 2000 highly variable genes were identified using the vst method for principal component analysis (PCA). The top 30 principal components were selected for further analysis. Finally, the FindNeighbors and Find Clusters algorithms (resolution = 0.5) from the Seurat package in R (version: 4.4.0) were used to cluster cells, followed by Uniform Manifold Approximation and Projection (UMAP) non-linear dimension reduction.

Cell annotation analysis

According to the cell types identified through clustering analysis, the FindAllMarkers function in the Seurat package was used to identify the hub genes for each cell type with cut-off values of adj.$P < 0.05$ and $|\log_2 FC| > 0.5$. The clustering-derived cell types were further annotated using the SingleR package in R (version: 2.4.1) (Aran *et al*., 2019) and the CellMarker database. The annotated cell populations were visualized using UMAP projections. A bubble plot was generated to illustrate the expression patterns of hub genes across annotated cell types.

Key cell identification

This study employed the PercentageFeatureSet function in the Seurat package to integrate the expression of RBRGs, thereby calculating the proportion of ribosomal synthesis genes expressed in individual cells. This approach facilitates the quantitative assessment of ribosomal gene expression relative to total cellular gene expression. The resulting expression proportions were then compared between different cell clusters, with a particular focus on evaluating the differential expression patterns between cancerous and adjacent non-cancerous tissues. Cells exhibiting a trend in ribosomal gene activity consistent with their transcriptomic profiles were selected as key cells for further analysis.

Statistical analysis

Statistical analyses were conducted in the R software (version: 4.3.3). Data distributions guided the selection of comparative methods: Wilcoxon rank-sum tests for non-normal distributions and Student's *t*-tests for normally distributed variables. Results achieving *P* values below 0.05 were considered statistically significant.

RESULTS

DE-RBRGs investigation

Using ssGSEA methodology, this study quantified the expression levels of 331 RBRGs using a GSVA score for each sample in TCGA dataset. Notably, hepatic tumor specimens exhibited markedly elevated GSVA scores compared to non-malignant tissues, indicating an important role for ribosomal synthesis in the development of HCC (Fig. 1A). Differential expression analysis identified 88 DE-RBRGs 76 up-regulated and 12 down-regulated genes) between HCC and normal samples (Fig. 1B). The heatmap analysis showed that all these genes could be distinctly separated by tissue type (Fig. 1C). Functional enrichment analysis showed that these DE-RBRGs mainly participated in GO functions such as ribosome biogenesis (BP, GO:0042254), peribosomes (CC, GO:0030684) and structural constituent of ribosome (MF, GO:0003735) (Fig. 1D). Pathway analysis further highlighted their involvement in ribosomal processes (hsa03010) (Fig. 1E). Molecular interactions among these DE-RBRGs were subsequently visualized using PPI analysis (Fig. 1F). The resulting network was comprised of 57 nodes (genes) and 440 interactions, with bystin like (BYSL), Ribosomal Protein S7 (RPS7) and Ribosomal Protein S16 (RPS16) emerging as potential core proteins owing to their high degrees of connectivity.

Screening of prognostic DE-RBRGs to construct a predictive model

The Cox regression analysis identified that a total of 12 DE-RBRGs including Interferon Stimulated Exonuclease Gene 20 Like 2 (*ISG20L2*), Drosha Ribonuclease III (*DROSHA*), *TCOF1*, Nucleophosmin 1 (*NPM1)*, Dyskerin Pseudouridine Synthase 1 (*DKC1)*, Protein Kinase, DNA-Activated, Catalytic Subunit (*PRKDC)*, DDB1 And CUL4 Associated Factor 13 (*DCAF13)*, RNA Terminal Phosphate Cyclase Like 1 (*RCL1)*, Ribosomal RNA Processing 12 Homolog (*RRP12)*, DEAD/H-Box Helicase 11 (*DDX11)*, Ras-Related Nuclear Protein (*RAN)* and NOP56 Ribonucleoprotein (*NOP56)* were closely associated with the prognosis of HCC, which were considered as prognostic genes in the current study (Fig.

2A). The interaction analysis using GeneMANIA showed that these prognostic genes were mainly assembled as functions of ribosome biogenesis and co-expression networks (Fig. 2B). We then evaluated 101 machine learning algorithms to identify the optimal strategy for constructing a prognostic model. The combination of StepCox [forward] + SuperPC demonstrated the best performance, achieving the highest average C-index of 0.66, 0.72 and 0.61 in TCGA, ICGC and GSE14520 datasets, respectively (Fig. 2C). Using the median risk score as a cutoff value, we stratified the samples into two risk groups. KM analysis in the training cohort revealed that patients in the high-risk group had significantly reduced survival compared to those in the low-risk group, a finding that was consistent with the results from the two validation datasets (Fig. 2D). Time-dependent ROC analysis demonstrated robust predictive accuracy, with area under the curve values of 0.723, 0.673 and 0.670 at the one-, three- and five-year intervals, respectively (Fig. 2E). Consistent predictive accuracy was observed in both the GSE14520 and ICGC datasets, further supporting the potential of this model for predicting HCC prognosis (Fig. 2E). In addition, meta-analysis was conducted on the training and validation datasets using univariate Cox regression (Fig. 2F). The results showed that current risk model was a risk factor for HCC either with random (hazard ratio [HR] = 2.26, 95% confidence interval [CI]: 1.75-2.92, $P < 0.001$) or fixed (HR = 2.26, 95% CI: 1.75-2.92, $P < 0.001$) effect models.

Prognostic model evaluation

Validation of these 12 prognostic genes showed that their expression trends of these prognostic genes in the training dataset were basically consistent with those in the two validation datasets (GSE14520 and GSE76427). Specifically, *RCL1* was down-regulated in the HCC samples, whereas *ISG20L2*, *DROSHA*, *TCOF1*, *NPM1*, *DKC1*, *PRKDC*, *RAN* and *NOP56* were up-regulated (Fig. 3A). Survival analysis of these 12 prognostic genes indicated that *DKC1* expression was not significantly associated with HCC prognosis. In contrast, low expression of *RCL1* correlated with a poor prognosis of HCC, whereas high expression of the remaining 10 genes was associated with worse clinical outcomes (Fig. 3B).

Immune landscape and drug sensitive analyses

With a significance threshold of $P < 0.05$, a total of eight immune cell types were differentially infiltrated between the two risk groups (Fig. 4A). Specifically, the infiltration levels of CD4 T cells, activated dendritic cells, natural killer T cells and T follicular helper cells in the low-risk group were dramatically lower than those in the high-risk group ($P < 0.001$). Conversely, effector memory CD8 T cells, eosinophils, natural killer cells and Type 1 helper cells showed significantly higher infiltration abundances in the low-risk group relative to the high-risk group ($P < 0.001$). The correlations between immune cells and the 12 prognostic genes are shown in Fig. 4B. Notably, the infiltration level of activated CD4 T cells was positively correlated with the expression of most prognostic genes, except for *RCL1*. In contrast, eosinophilic infiltration was negatively correlated with these prognostic genes, except for *RCL1*. TIDE metric evaluation revealed distinct immune evasion patterns between the risk groups (Fig. 4C). Patients in the low-risk group demonstrated reduced TIDE indices, indicating a greater likelihood of benefitting from immunotherapy. Immune checkpoint analysis revealed elevated expression of multiple checkpoint molecules in high-risk patients compared with their low-risk counterparts (Fig. 4D). Genomic analysis identified characteristic mutation profiles of the top 20 most frequently mutated genes in each risk group, as illustrated in figs. 4E. The result showed that *CTNNB1* and *TP53* mutations had the highest frequencies in the low- and high-risk groups, respectively (Fig. 4E). Finally, drug sensitivity analysis showed that the up-regulation of almost all prognostic genes influenced patient responsiveness to targeted drugs such as Gefitinib and RDEA119 (Fig. 4F).

Single-cell investigation

Single-cell data from the GSE149614 dataset were initially preprocessed for QC. Consequently, a total of 25,479 genes and 60,504 cells were retained for subsequent analysis (Fig. S1A-B). Highly variable gene analysis revealed the top 10 most variable genes, including Immunoglobulin Alpha 1 (*IGHA1*), Tryptase Alpha/Beta 1 (*TPSAB1*) and C-C Motif Chemokine Ligand 26 (*CCL26*) (Fig. S1C). Then, PCA revealed a uniform sample distribution along the two principal components (PCs), with no evident batch effects or outliers, indicating minimal variation between samples, minimal intersample variation and high data reproducibility (Fig. 5A). Linear dimensionality reduction analysis demonstrated a turning point (“elbow”) in PC 30, indicating that the top 30 PCs captured the majority of biological variation (Fig. 5B). These 30 PCs were used for cell clustering based on the UMAP nonlinear dimensionality reduction, which resolved 23 distinct cell clusters (Fig. 5C). Following, a total of nine cell types were annotated as follows: NK cells, T cells, B cells, fibroblasts, macrophages, endothelial cells, proliferative cells, hepatocytes and plasma cells (Fig. 5D). The expression patterns of marker genes in different cell types are shown in Fig. 5E. Notably, Albumin (*ALB*) and Transthyretin (*TTR*) were highly expressed in the hepatocytes. Comparative cellular profiling demonstrated distinct compositional variations in hepatocytes, T cells, NK cells, B cells and proliferative cells between malignant tissues and the surrounding non-tumor specimens (Fig. 5F).

Key cell investigation

This study further calculated the ribosomal scores for individual cells based on the expression of RBRGs. Comparative analysis revealed significant differences in ribosomal scores between HCC and normal tissues across all annotated cell types, except for fibroblasts (Fig. 6A).

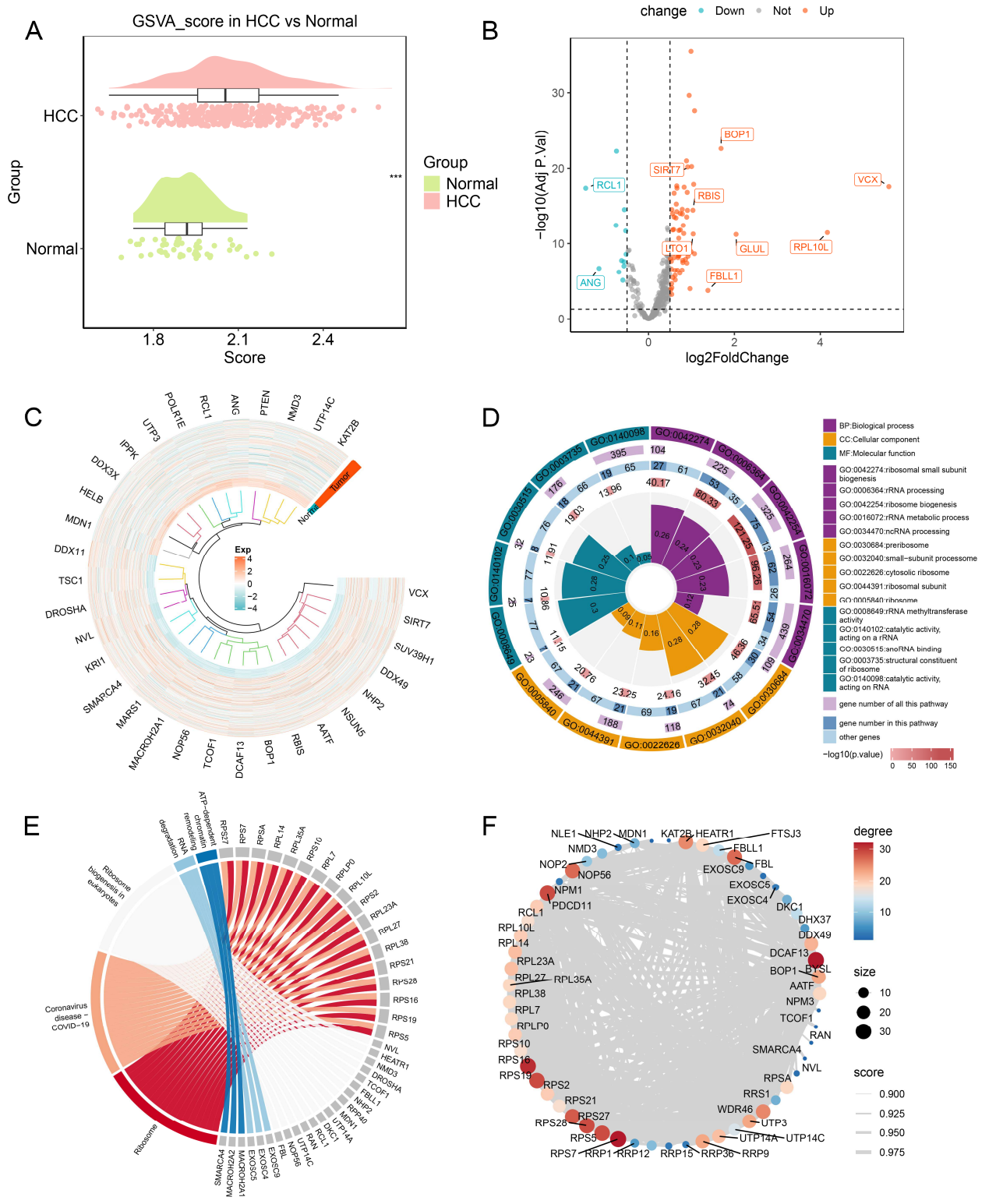

Fig. 1: The investigation for differentially expressed (DE) ribosome biogenesis-related genes (RBRGs).
(A) The difference in GSVA score between hepatocellular carcinoma (HCC) and normal groups based on expression profiles of RBRGs. ***$P < 0.001$; (B) The volcano plot showed the DE-RBRGs between HCC and normal samples; (C) The heatmap analysis showing expression pattern difference of DE-RBRGs between HCC and normal samples; (D-E) The significant GO functions (D) and KEGG pathways (E) enriched by DE-RBRGs; (F) The protein-protein interaction (PPI) network constructed by DE-RBRGs.

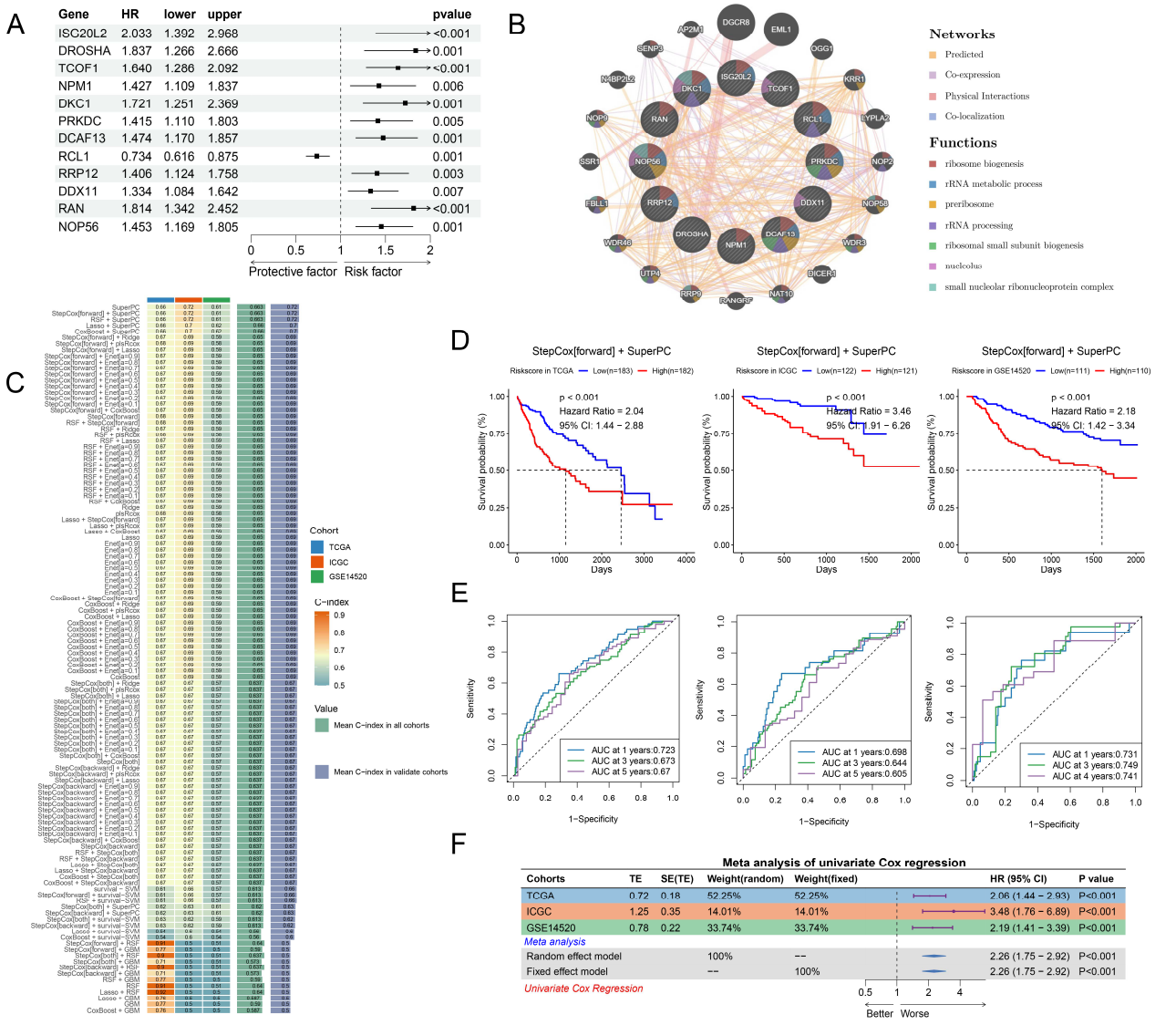

Fig. 2: Screening of prognostically differentially expressed (DE) ribosome biogenesis-related genes (RBRGs) to construct a predictive model.

(A) The forest plot showed the result of univariate Cox regression analysis, revealing 12 DE-RBRGs with prognostic values in hepatocellular carcinoma (HCC); (B) The interaction network analysis on 12 prognostic genes using GeneMANIA analysis; (C) The selection of optimal approach from 101 advanced machine learning algorithms to construct a predictive model; (D) KM survival analysis for current prognostic model constructed by 12 prognostic genes in training (TCGA: left panel) and validation (ICGC: middle panel; GSE14520: right panel) datasets; (E) The ROC analysis in both training (TCGA: left panel) and validation (GSE14520: middle panel; ICGC: right panel) datasets; (F) The meta-analysis revealed the relations between the prognostic model and HCC prognosis.

After integrating the differences in cell distribution and single-cell ribosomal scores between HCC and normal samples, we selected hepatocytes as the key cells for subsequent analysis (Fig. 6B). Moreover, the enrichment analysis performed on key cells showed that hepatocytes were primarily associated with up-regulated mTORC1 signaling and down-regulated TNF-α/NF-κB signaling pathways (Fig. 6C). The expression of prognostic genes in the hepatocytes is shown in Fig. 6D. The results demonstrated that the prognostic genes, *NPM1* and *RAN*, were highly expressed in hepatocytes.

DISCUSSION

Although ribosome biogenesis mechanisms are well-established to be critically involved in the initiation and progression of human malignancies (Elhamamsy *et al.*, 2022), the specific role and prognostic significance of RBRG in HCC remain poorly understood. In this study, a comprehensive analysis of single-cell and bulk RNA sequencing data identified 12 RBRGs (*ISG20L2*, *DROSHA*, *TCOF1*, *NPM1*, *DKC1*, *PRKDC*, *DCAF13*, *RCL1*, *RRP12*, *DDX11*, *RAN* and *NOP56*) significantly associated with HCC prognosis.

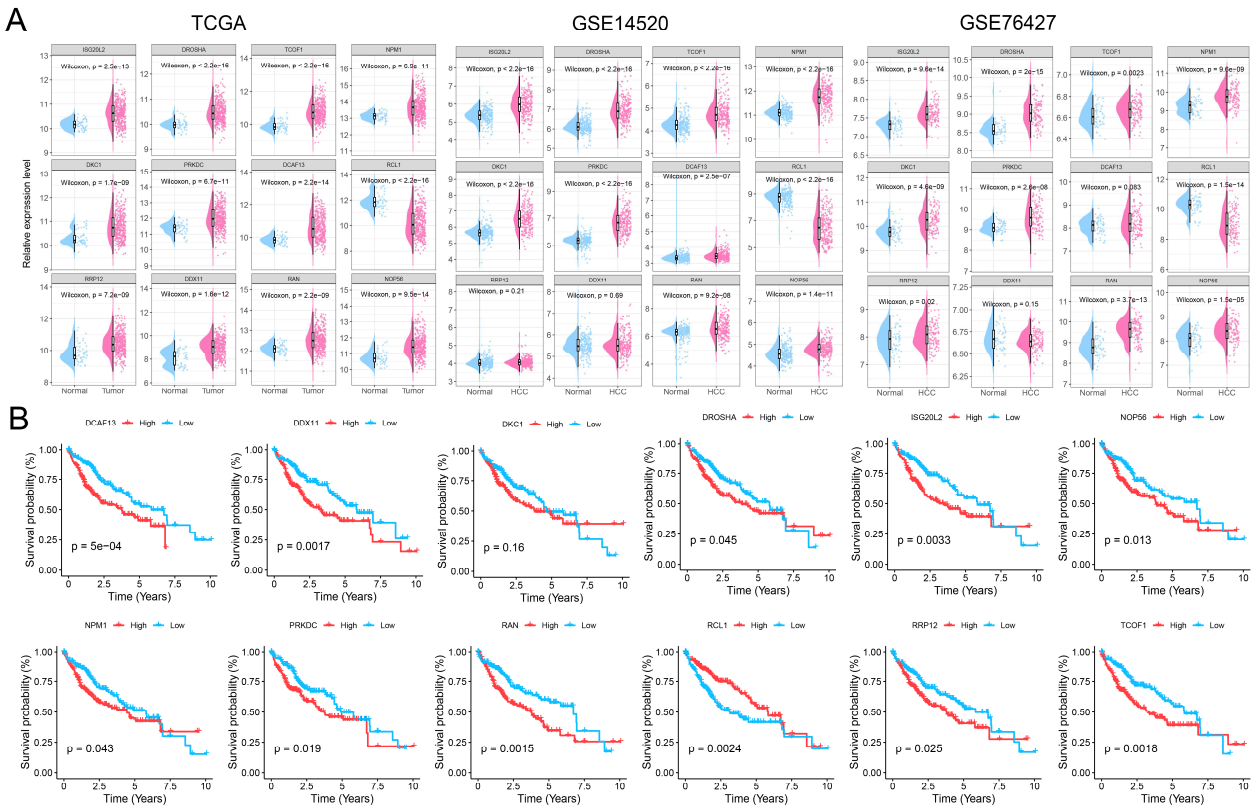

Fig. 3: Validating the expression pattern and survival relevance of 12 prognostic genes.
(A) The expression validation of 12 prognostic genes in TCGA, GSE14520, and GSE76427 datasets; (B) The survival analysis for 12 prognostic genes.

The prognostic model developed from these 12 RBRGs could predict prognostic risks of HCC. Moreover, hepatocytes may contribute to HCC pathogenesis through the upregulation of key prognostic genes (*NPM1* and *RAN*).

The identification of RBRGs as prognostic biomarkers in HCC has significant clinical implications, because their aberrant regulation is closely linked to the pathogenesis of multiple malignancies (Yang *et al*., 2023). Nucleolar morphological alterations may enhance ribosome biogenesis and protein translation, thereby promoting cancer aggressiveness through increased cell proliferation, migration and invasion (Saffarian *et al*., 2025). Among the 12 prognostic genes identified in our study, *NPM1* is a multifunctional nucleolar protein that plays crucial roles in cell proliferation, genome stability and cell cycle regulation (Falini, 2023). In HCC, aberrant expression and localization of NPM1 have been proven to be closely associated with tumor progression, prognosis and chemotherapeutic resistance (Zhang *et al*., 2022). *RAN*, a member of the RAS oncogene family, is also overexpressed in HCC and is closely associated with a poor prognosis (Elsalahaty *et al*., 2023). *RRP12* plays a role in the processing of ribosomal RNA and affects the occurrence and progression of liver cancer by modulating protein synthesis and cell cycle regulation (Wei *et al*., 2022). Consistent with these findings, our study revealed that all 12 identified RBRGs exhibited significant prognostic values in HCC risk stratification. Among these, *NPM1*, *RAN* and *RRP12* have been identified as risk factors for HCC. Moreover, these 12 RBRGs were mainly assembled for functions such as ribosome biogenesis. A similar HCC prognostic model was established by Grinchuk *et al*., who identified a ribosome-associated molecular signature that predicts clinical outcomes in surgically treatable hepatic carcinoma (Grinchuk *et al*., 2018). However, our study advances this field through integrative analysis of bulk RNA and single-cell sequencing data, providing novel insights into how nuclear ribosome biogenesis cooperates with the immune microenvironment to drive HCC progression. Therefore, the clinical application of this model could provide more personalized prognostic assessment for patients with HCC.

The immune microenvironment has been demonstrated to play a critical role in cancer progression (Yang *et al*., 2023). In this study, the CD4+ T cells were highly infiltrated in HCC samples and positively correlated with *RAN*, *DDX11*, *TCOF1*, and *NOP56*, but negatively correlated with *RCL1*, suggesting a potential involvement of these genes in the tumor immune microenvironment.

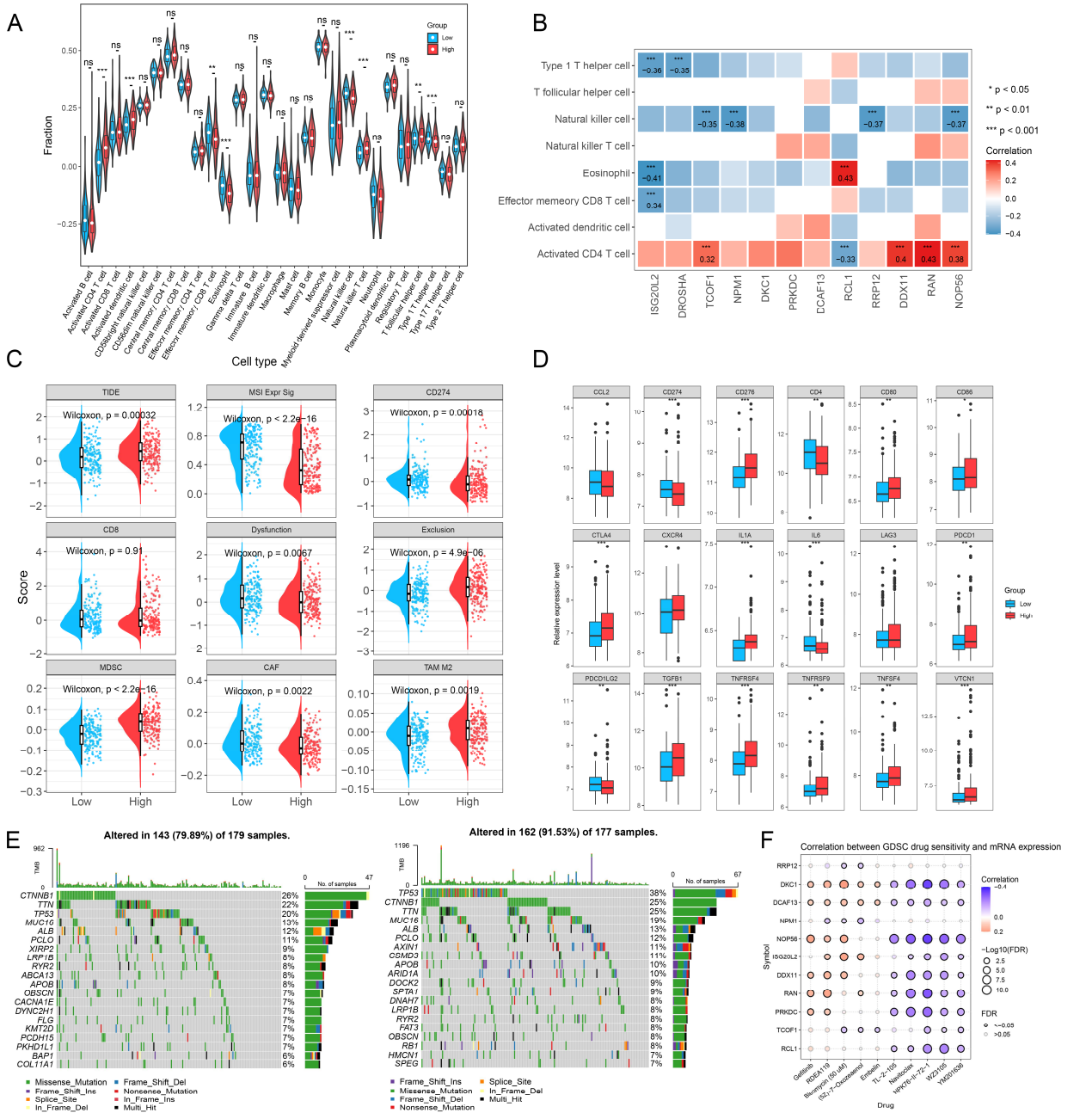

Fig. 4: Immune landscape, tumor mutation burden, and drug sensitivity investigation based on tumor samples between high-risk and low-risk groups.
(A) immune infiltration analysis revealing significant differential proportions of eight types of immune cells between risk groups; (B) Correlations between infiltrating immune cells and expression of prognostic genes; (C) Differences in TIDE scores between the two risk groups; (D) The expression differences of immune checkpoints between high-risk and low-risk groups; (E) Gene mutation analysis in high-risk and low-risk groups; (F) Correlations between prognostic genes and drug sensitivity in two risk groups. *$P < 0.05$; **$P < 0.01$; ***$P < 0.001$; ****$P < 0.0001$.

A previous study has highlighted the significant role of *RAN* in immune cell regulation, particularly during T cell activation (Che *et al*., 2021). The observed positive association between *RAN* and activated CD4 T cells in our study may imply its contribution to tumor immune responses, potentially influencing tumor immune evasion by modulating T cell activation and function. *TCOF1* coordinates oncogenic activation and rRNA production and promotes tumorigenesis in HCC (Wu *et al*., 2022). Interestingly, *TCOF1* expression was significantly correlated with CD4+ T cells in 16 cancer types including HCC (Gu *et al*., 2022).

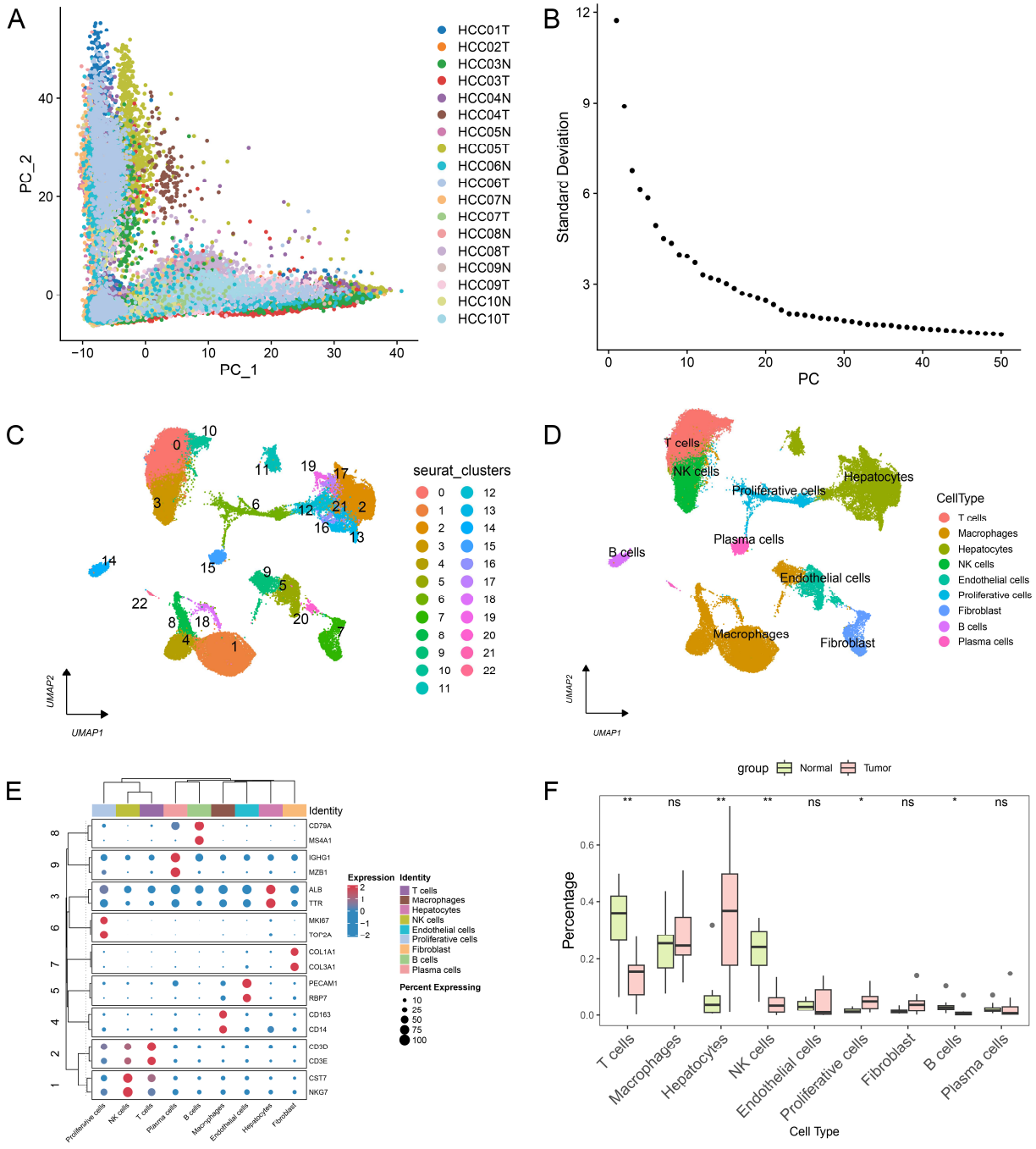

Fig. 5: Distribution of single cells in hepatocellular carcinoma (HCC) and normal samples.
(A) The result of linear dimension reduction via Principal Component Analysis (PCA); (B) The top 30 principal components (PCs) captured the majority of biological variation in PCA; (C) The Uniform Manifold Approximation and Projection (UMAP) non-linear dimension reduction on all samples; (D) Distribution of nine annotated cell types; (E) The expression of marker genes in nine annotated cell types; (F) The distribution difference of annotated cells between HCC and normal samples. *$P < 0.05$; **$P < 0.01$.

Therefore, we speculate that *TCOF1* may promote HCC tumorigenesis by activating the infiltration of CD4+ T cells through rRNA production. These findings provide new insights into the role of RBRGs in the immune microenvironment and highlight their potential as therapeutic targets for immunotherapy.

Single-cell analysis in this study revealed key insights into the potential regulatory mechanisms of hepatocytes in HCC, with particular emphasis on the correlations between up-regulated *NPM1* and *RAN*. Hepatocytes undergo dedifferentiation and acquire stem cell-like properties that contribute to tumor growth and metastasis (Liu *et al*., 2022).

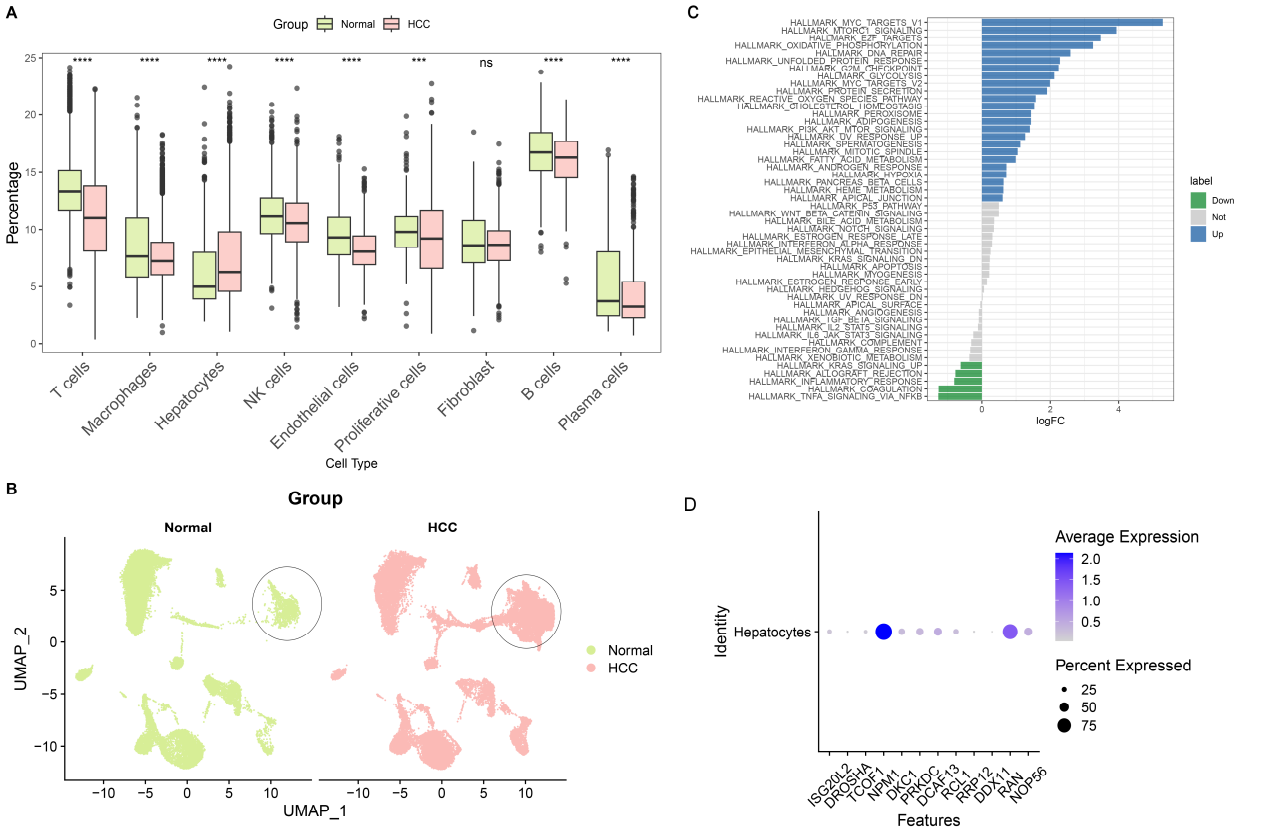

Fig. 6: The key cell investigation.
(A) differences in ribosome scores of annotated cells between groups. ****$P < 0.0001$; (B) The distribution differences of annotated cells between HCC and normal groups; (C) The enrichment analysis for key cell hepatocytes; (D) The expression of prognostic genes in the hepatocytes.

The dysregulation of ribosomal gene expression in hepatocytes further supports the idea that increased ribosome biogenesis is essential for the rapid proliferation characteristic of cancer cells (Yang *et al*., 2023). *NPM1*, a nucleolar protein involved in RNA synthesis and cell cycle regulation, exhibits elevated expression in hepatocytes, which is consistent with its association with poor prognosis in HCC and other malignancies (Liu *et al*., 2012). A previous study highlighted the role of *NPM1* in promoting tumor cell proliferation. Furthermore, targeting *NPM1* inhibited proliferation and induced apoptosis in hepatic progenitor cells by suppressing the mTOR signaling pathway (Wang *et al*., 2024a). In HCC, up-regulated mTORC1 may contribute to tumor growth and expansion, while the down-regulated coagulation pathway may reflect changes in the tumor microenvironment that promote metastasis and immune evasion (Yu *et al*., 2023b). Our analysis revealed that hepatocytes were enriched in the mTORC1 signaling pathway, which supports cell growth and metabolism in HCC (Zhu *et al*., 2022). Additionally, RAN translation is closely linked to ribosome synthesis (Neueder and Bates, 2018). Studies have shown that ribosome stalling and activation of the RQC pathway can suppress the formation of toxic RAN products (Tseng *et al*., 2024). RAN serves as a reliable biomarker for HCC and, along with other prognostic genes, functions as a classifier to predict HCC prognosis (Nault *et al*., 2013, Hai *et al*., 2024). Notably, RAN expression is suppressed by PI3K/mTOR inhibitors (Wang *et al*., 2025), suggesting coordinated expression between RAN and the mTOR pathway in HCC hepatocytes. Our single-cell analysis showed that two prognostic genes, *NPM1* and *RAN*, were highly expressed in hepatocytes. In addition, key hepatocytes activate the mTORC1 signaling pathway. These findings collectively suggest that hepatocytes may play a pivotal role in HCC development through the regulation of *NPM1* and *RAN* and the activation of the mTORC1 signaling pathway, providing new insights into the molecular mechanisms underlying HCC progression.

This study has several limitations that should be acknowledge. First, although the reliability of the model across multiple cohorts was validated, the relatively limited sample size may constrain the generalizability of our findings. Second, although single-cell analysis revealed the heterogeneity of hepatocytes, an in-depth mechanistic exploration of hepatocyte function and immune responses remains to be fully elucidated. Thirdly, the expression

patterns and prognostic correlations of these RBRGs lack robust experimental and clinical evidences. Future studies should use independent clinical cohorts and experimental methodologies to further validate these findings. Additionally, exploring combinatory strategies that target ribosome synthesis pathways in conjunction with immunotherapy may facilitate the development of personalized treatment options for patients with HCC.

CONCLUSION

In summary, this study highlights the significance of a 12-RBRG-based prognostic model for HCC and identifies promising biomarkers for potential therapeutic applications. Moreover, hepatocytes may contribute to HCC progression by up-regulating *NPM1* and *RAN* and activating the mTORC1 signaling pathway.

Acknowledgements
We thank Anjing Zhao for conducting the mentioned literature research and subsequent data analysis. Thanks are due to Chunming Wu for detailed revision guidance on the completed first draft of the writing.

Authors' contribution
ChunmingWu: Conception and design of the research; Jingjing Feng and Linrong Zhu: Acquisition of data; Qianqian Hu: Analysis and interpretation of data; Jinglian Zheng: Statistical analysis; Anjing Zhao: Drafting the manuscript; Chunming Wu: Revision of manuscript for important intellectual content. All authors read and approved the final manuscript.

Funding
This research received no external funding.

Data availability statement
The datasets used and/or analyzed during the current study are available from the corresponding author on reasonable request.

Ethical approval
This study does not involve human participants or animals. Therefore, ethical approval is not applicable.

Conflict of interest
The authors declare no conflict of interest.

Supplementary data
https://www.pjps.pk/uploads/2026/04/SUP1776948827.pdf

REFERENCES

Aran D, Looney AP, Liu L, Wu E, Fong V, Hsu A, Chak S, Naikawadi RP, Wolters PJ, Abate AR, Butte AJ and Bhattacharya M (2019). Reference-based analysis of lung single-cell sequencing reveals a transitional profibrotic macrophage. *Nat. Immunol.,* **20**(2): 163-172.

Brown ZJ, Tsilimigras DI, Ruff SM, Mohseni A, Kamel IR, Cloyd JM and Pawlik TM (2023). Management of hepatocellular carcinoma: A review. *JAMA Surg.,* **158**(4): 410-420.

Cao K, Wang R, Li L, Liao Y, Hu X, Li R, Liu X, Xiong XD, Wang Y and Liu X (2024). Targeting DDX11 promotes PARP inhibitor sensitivity in hepatocellular carcinoma by attenuating BRCA2-RAD51 mediated homologous recombination. *Oncogene,* **43**(1): 35-46.

Chan YT, Zhang C, Wu J, Lu P, Xu L, Yuan H, Feng Y, Chen ZS and Wang N (2024). Biomarkers for diagnosis and therapeutic options in hepatocellular carcinoma. *Mol Cancer,* **23**(1): 189.

Che X, Liu M, Li D, Li Z, Guo J and Jia R (2021). RAN and YBX1 are required for cell proliferation and IL-4 expression and linked to poor prognosis in oral squamous cell carcinoma. *Exp. Cell Res.,* **406**(2): 112767.

Chen Y, Li Y, Xiong J, Lan B, Wang X, Liu J, Lin J, Fei Z, Zheng X and Chen C (2021). Role of PRKDC in cancer initiation, progression and treatment. *Cancer Cell Int.,* **21**(1): 563.

Dopazo C, Søreide K, Rangelova E, Mieog S, Carrion-Alvarez L, Diaz-Nieto R, Primavesi F and Stättner S (2024). Hepatocellular carcinoma. *Eur. J. Surg. Oncol.,* **50**(1): 107313.

Elhamamsy AR, Metge BJ, Alsheikh HA, Shevde LA and Samant RS (2022). Ribosome biogenesis: A central player in cancer metastasis and therapeutic resistance. *Cancer Res.,* **82**(13): 2344-2353.

Elsalahaty MI, Salama AF, Diab T, Ghazy M, Toraih E and Elshazli RM (2023). Unleash multifunctional role of miRNA biogenesis gene variants (XPO5*rs34324334 and RAN*rs14035) with susceptibility to hepatocellular carcinoma. *J. Pers. Med.,* **13**(6): 959.

Falini B (2023). NPM1-mutated acute myeloid leukemia: New pathogenetic and therapeutic insights and open questions. *Am. J. Hematol.,* **98**(9): 1452-1464.

Grinchuk OV, Yenamandra SP, Iyer R, Singh M, Lee HK, Lim KH, Chow PK and Kuznetsov VA (2018). Tumor-adjacent tissue co-expression profile analysis reveals pro-oncogenic ribosomal gene signature for prognosis of resectable hepatocellular carcinoma. *Mol. Oncol.,* **12**(1): 89-113.

Gu W, Sun L, Wang J and Chen X (2022). The oncogenic role of treacle ribosome biogenesis factor 1 (TCOF1) in human tumors: A pan-cancer analysis. *Aging (Albany NY),* **14**(2): 943-960.

Guo S, Nguyen L and Ranum LPW (2022). RAN proteins in neurodegenerative disease: Repeating themes and unifying therapeutic strategies. *Curr. Opin. Neurobiol.,* **72**: 160-170.

Hai L, Bai XY, Luo X, Liu SW, Ma ZM, Ma LN and Ding XC (2024). Prognostic modeling of hepatocellular

carcinoma based on T-cell proliferation regulators: A bioinformatics approach. *Front. Immunol.,* **15**: 1444091.

Ji X, Yang Z, Li C, Zhu S, Zhang Y, Xue F, Sun S, Fu T, Ding C, Liu Y and Wan Q (2024). Mitochondrial ribosomal protein L12 potentiates hepatocellular carcinoma by regulating mitochondrial biogenesis and metabolic reprogramming. *Metabolism,* **152**: 155761.

Jiaze Y, Sinan H, Minjie Y, Yongjie Z, Nan D, Liangwen W, Wen Z, Jianjun L and Zhiping Y (2022). Rcl1 suppresses tumor progression of hepatocellular carcinoma: A comprehensive analysis of bioinformatics and *in-vitro* experiments. *Cancer Cell Int.,* **22**(1): 114.

Kim J, Huang K, Vo PTT, Miao T, Correia J, Kumar A, Simons MJP and Bai H (2024). Peroxisomal import stress activates integrated stress response and inhibits ribosome biogenesis. *PNAS Nexus,* **3**(10): 429.

Ko E, Kim JS, Ju S, Seo HW, Chang Y, Kang JA, Park SG and Jung G (2018). Oxidatively modified protein-disulfide isomerase-associated 3 promotes dyskerin pseudouridine synthase 1-mediated malignancy and survival of hepatocellular carcinoma cells. *Hepatology,* **68**(5): 1851-1864.

Li Y, Jiang M, Wei Y, He X, Li G, Lu C and Ge D (2024). Integrative analyses of pyrimidine salvage pathway-related genes revealing the associations between UPP1 and tumor microenvironment. *J. Inflamm. Res.,* **17**: 101-119.

Liu H, Zhang W, Zhang Y, Adegboro AA, Fasoranti DO, Dai L, Pan Z, Liu H, Xiong Y, Li W, Peng K, Wanggou S and Li X (2024). Mime: A flexible machine-learning framework to construct and visualize models for clinical characteristics prediction and feature selection. *Comput. Struct. Biotechnol. J.,* **23**: 2798-2810.

Liu J, Geng W, Sun H, Liu C, Huang F, Cao J, Xia L, Zhao H, Zhai J, Li Q, Zhang X, Kuang M, Shen S, Xia Q, Wong VW and Yu J (2022). Integrative metabolomic characterisation identifies altered portal vein serum metabolome contributing to human hepatocellular carcinoma. *Gut.,* **71**(6): 1203-1213.

Liu TT, Li R, Huo C, Li JP, Yao J, Ji XL and Qu YQ (2021a). Identification of CDK2-related immune forecast model and ceRNA in lung adenocarcinoma, a pan-cancer analysis. *Front Cell Dev. Biol.,* **9**: 682002.

Liu X, Liu D, Qian D, Dai J, An Y, Jiang S, Stanley B, Yang J, Wang B, Liu X and Liu DX (2012). Nucleophosmin (NPM1/B23) interacts with activating transcription factor 5 (ATF5) protein and promotes proteasome- and caspase-dependent ATF5 degradation in hepatocellular carcinoma cells. *J. Biol. Chem.,* **287**(23): 19599-609.

Liu Z, Pang Y, Jia Y, Qin Q, Wang R, Li W, Jing J, Liu H and Liu S (2021b). SNORA23 inhibits HCC tumorigenesis by impairing the 2'-O-ribose methylation level of 28S rRNA. *Cancer Biol. Med.,* **19**(1): 104-19.

Love MI, Huber W and Anders S (2014). Moderated estimation of fold change and dispersion for RNA-seq data with DESeq2. *Genome Biol.,* **15**(12): 550.

Luo Y, Lin J, Zhang Y, Dai G, Li A and Liu X (2020). LncRNA PCAT6 predicts poor prognosis in hepatocellular carcinoma and promotes proliferation through the regulation of cell cycle arrest and apoptosis. *Cell Biochem. Funct.,* **38**(7): 895-904.

Nault JC, De Reyniès A, Villanueva A, Calderaro J, Rebouissou S, Couchy G, Decaens T, Franco D, Imbeaud S, Rousseau F, Azoulay D, Saric J, Blanc JF, Balabaud C, Bioulac-Sage P, Laurent A, Laurent-Puig P, Llovet JM and Zucman-Rossi J (2013). A hepatocellular carcinoma 5-gene score associated with survival of patients after liver resection. *Gastroenterology,* **145**(1): 176-187.

Neueder A and Bates GP (2018). RNA Related Pathology in Huntington's Disease. *Adv. Exp. Med. Biol.,* **1049**: 85-101.

Ni C and Buszczak M (2023). Ribosome biogenesis and function in development and disease. *Development,* **150**(5): dev201187.

Pan Y, Zhu Q, Hong T, Cheng J and Tang X (2024). Targeting PRKDC activates the efficacy of antitumor immunity while sensitizing to chemotherapy and targeted therapy in liver hepatocellular carcinoma. *Aging (Albany NY),* **16**(10): 9047-9071.

Rosell-Díaz M, Petit-Gay A, Molas-Prat C, Gallardo-Nuell L, Ramió-Torrentà L, Garre-Olmo J, Pérez-Brocal V, Moya A, Jové M, Pamplona R, Puig J, Ramos R, Bäckhed F, Mayneris-Perxachs J and Fernández-Real JM (2024). Metformin-induced changes in the gut microbiome and plasma metabolome are associated with cognition in men. *Metabolism,* **157**: 155941.

Roy SK, Srivastava S, Mccance C, Shrivastava A, Morvant J, Shankar S and Srivastava RK (2024). Clinical significance of PNO1 as a novel biomarker and therapeutic target of hepatocellular carcinoma. *J. Cell Mol. Med.,* **28**(9): e18295.

Saffarian S, Cai Z, Lam J, Oo HZ and Somasekharan S (2025). Elevated NPM1 and FBL expression correlates with prostate cancer aggressiveness and progression. *J. Pathol*, **267**(1): 56-68.

Su SG, Li QL, Zhang MF, Zhang PW, Shen H and Zhang CZ (2020). An E2F1/DDX11/EZH2 positive feedback loop promotes cell proliferation in hepatocellular carcinoma. *Front Oncol.,* **10**: 593293.

Szklarczyk D, Morris JH, Cook H, Kuhn M, Wyder S, Simonovic M, Santos A, Doncheva NT, Roth A and Bork P (2016). The STRING database in 2017: Quality-controlled protein–protein association networks, made broadly accessible. *Nucleic acids research*, **45**(D1): D362-D368.

Tseng YJ, Krans A, Malik I, Deng X, Yildirim E, Ovunc S, Tank EMH, Jansen-West K, Kaufhold R, Gomez NB, Sher R, Petrucelli L, Barmada SJ and Todd PK (2024). Ribosomal quality control factors inhibit repeat-associated non-AUG translation from GC-rich repeats. *Nucleic. Acids Res.,* **52**(10): 5928-5949.

Wang D, Yang Q, Zhu G, Li Z, Wu C, Hu X, Long G, Wang Q, Chen Y, Xu C, Huang C, Han Y and Zhang D (2025). Voxtalisib inhibits enterovirus 71 replication by downregulating host RAN and restoring IFN-STAT signaling. *J. Adv. Res*., **81**: 569-582.

Wang P, Wang M, Liu L, Li H, Liu H, Ren J, Liu T, Cong M, Zhu Z, Zhao X, Sun L and Jia J (2024a). Targeting NPM1 inhibits proliferation and promotes apoptosis of hepatic progenitor cells via suppression of mTOR signalling pathway. *Stem. Cell Res. Ther.,* **15**(1): 292.

Wang X, Zhang XY, Liao NQ, He ZH and Chen QF (2024b). Identification of ribosome biogenesis genes and subgroups in ischaemic stroke. *Front Immunol.,* **15**: 1449158.

Wang Y and Deng B (2023). Hepatocellular carcinoma: Molecular mechanism, targeted therapy and biomarkers. *Cancer Metastasis Rev.,* **42**(3): 629-652.

Warde-Farley D, Donaldson SL, Comes O, Zuberi K, Badrawi R, Chao P, Franz M, Grouios C, Kazi F and Lopes CT (2010). The GeneMANIA prediction server: Biological network integration for gene prioritization and predicting gene function. *Nucleic. acids research,* **38**: W214-W220.

Wei C, Wang B, Chen ZH, Xiao H, Tang L, Guan JF, Yuan RF, Yu X, Hu ZG, Wu HJ, Dai Z and Wang K (2022). Validating RRP12 expression and its prognostic significance in hcc based on data mining and bioinformatics methods. *Front Oncol.,* **12**: 812009.

Wu B, Liu DA, Guan L, Myint PK, Chin L, Dang H, Xu Y, Ren J, Li T, Yu Z, Jabban S, Mills GB, Nukpezah J, Chen YH, Furth EE, Gimotty PA, Wells RG, Weaver VM, Radhakrishnan R, Wang XW and Guo W (2023). Stiff matrix induces exosome secretion to promote tumour growth. *Nat. Cell Biol.,* **25**(3): 415-424.

Wu C, Xia D, Wang D, Wang S, Sun Z, Xu B and Zhang D (2022). TCOF1 coordinates oncogenic activation and rRNA production and promotes tumorigenesis in HCC. *Cancer Sci.,* **113**(2): 553-564.

Wu T, Hu E, Xu S, Chen M, Guo P, Dai Z, Feng T, Zhou L, Tang W, Zhan L, Fu X, Liu S, Bo X and Yu G (2021). ClusterProfiler 4.0: A universal enrichment tool for interpreting omics data. *Innovation (Camb),* **2**(3): 100141.

Xiao B, Liu L, Li A, Xiang C, Wang P, Li H and Xiao T (2020). Identification and verification of immune-related gene prognostic signature based on ssGSEA for osteosarcoma. *Front Oncol.,* **10**: 607622.

Yang XM, Wang XQ, Hu LP, Feng MX, Zhou YQ, Li DX, Li J, Miao XC, Zhang YL, Yao LL, Nie HZ, Huang S, Xia Q, Zhang XL, Jiang SH and Zhang ZG (2023). Nucleolar HEAT repeat containing 1 up-regulated by the mechanistic target of rapamycin complex 1 signaling promotes hepatocellular carcinoma growth by dominating ribosome biogenesis and proteome homeostasis. *Gastroenterology,* **165**(3): 629-646.

Yu G, Xu S, Kong J, He J and Liu J (2023a). Development and validation of web calculators to predict early recurrence and long-term survival in patients with duodenal papilla carcinoma after pancreaticoduodenectomy. *BMC Cancer,* **23**(1): 1129.

Yu J, Ling S, Hong J, Zhang L, Zhou W, Yin L, Xu S, Que Q, Wu Y, Zhan Q, Bao J, Xu N, Liu Y, Chen K, Wei X, Liu Z, Feng T, Zhou L, Xie H, Wang S, Liu J, Zheng S and Xu X (2023b). TP53/mTORC1-mediated bidirectional regulation of PD-L1 modulates immune evasion in hepatocellular carcinoma. *J. Immunother. Cancer,* **11**(11): e007479.

Zang Y, Ran X, Yuan J, Wu H, Wang Y, Li H, Teng H and Sun Z (2024). Genomic hallmarks and therapeutic targets of ribosome biogenesis in cancer. *Brief Bioinform,* **25**(2): 1-13.

Zhang D, Wu F, Song J, Meng M, Fan X, Lu C, Weng Q, Fang S, Zheng L, Tang B, Yang Y, Tu J, Xu M, Zhao Z and Ji J (2022). A role for the NPM1/PTPN14/YAP axis in mediating hypoxia-induced chemoresistance to sorafenib in hepatocellular carcinoma. *Cancer Cell Int.,* **22**(1): 65.

Zhang Q, Liu X, Zou Z and Zhou B (2023a). Evidence from a meta-analysis for the prognostic and clinicopathological importance of DKC1 in malignancies. *Future Oncol.,* **19**(6): 473-484.

Zhang S, Li X, Zheng Y, Liu J, Hu H, Zhang S and Kuang W (2023b). Single cell and bulk transcriptome analysis identified oxidative stress response-related features of Hepatocellular carcinoma. *Front Cell Dev. Biol.,* **11**: 1191074.

Zhao S, Zhang D, Liu S and Huang J (2023). The roles of NOP56 in cancer and SCA36. *Pathol. Oncol. Res.,* **29**: 1610884.

Zhou W, Chen Y, Luo R, Li Z, Jiang G and Ou X (2021). Identification of biomarkers related to immune cell infiltration in hepatocellular carcinoma using gene co-expression network. *Pathol. Oncol. Res.,* **27**: 601693.

Zhou W, Lin L, Chen D, Wang J and Chen J (2024). Construction of a liver cancer prognostic model based on interferon-gamma-related genes for revealing the immune landscape. *J. Environ. Pathol. Toxicol. Oncol.,* **43**(4): 25-42.

Zhu J, Wang H and Jiang X (2022). mTORC1 beyond anabolic metabolism: Regulation of cell death. *J. Cell Biol.,* **221**(12): e202208103.